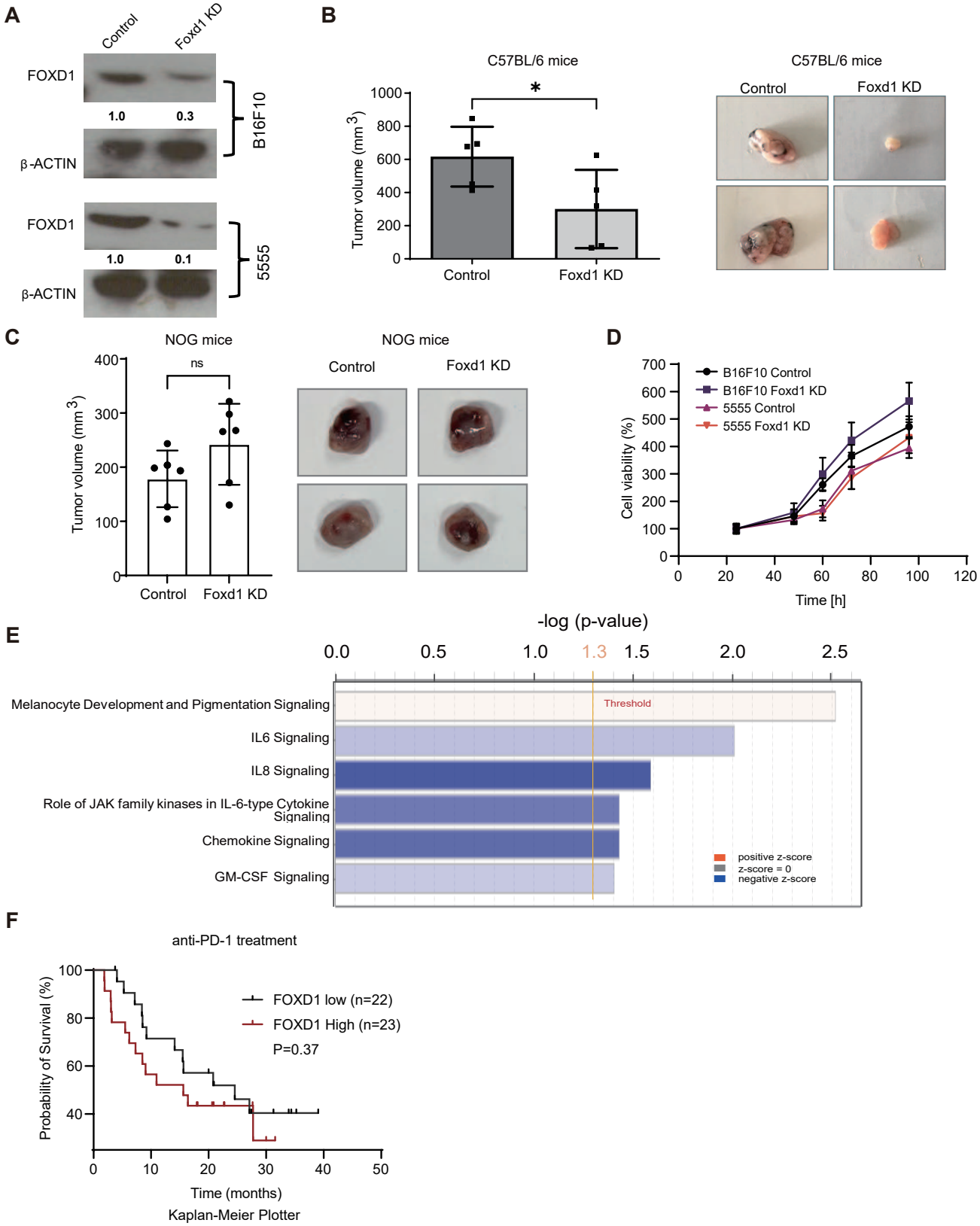

online supplemental figure 1. High FOXD1 expression in melanoma cells is associated with tumor progression.

(A) Western blot analysis of FOXD1 expression in FOXD1 KD and control murine melanoma cells. Densitometric values were normalized to the loading control β-ACTIN. (B) Left: Quantification of the tumor volume upon subcutaneous injection of 1×10^6 FOXD1 KD or control 5555 murine melanoma cells into C57BL/6 mice. The tumor volume was measured at day 14. Right: Representative images of excised tumors at day 14 from the FOXD1 KD and control group. (C) Ingenuity Pathway Analysis (IPA) showing the deactivation of several signaling pathways related to innate immunity and MDSC enrichment upon silencing FOXD1. IPA prediction was ranked based on the activation z-score. A positive score (red) denotes activation, while a negative score (blue) denotes inhibition. (D) Cell viability of FOXD1 KD and control murine melanoma cells in different time points (24 h-96 h) was analyzed using the Alamar Blue assay. (n=4). (E) Ingenuity Pathway Analysis (IPA) showing the deactivation of several signaling pathways related to innate immunity and MDSC enrichment upon silencing FOXD1. IPA prediction was ranked based on the activation z-score. A positive score (red) denotes activation, while a negative score (blue) denotes inhibition. (F) Survival of melanoma patients undergoing anti-PD1 treatment in relation to intratumoral FOXD1 expression. Results were generated using Kaplan-Meier Plotter online tool. Statistical analysis was performed with student's two-sided t-test. *P < 0.05; **P < 0.01; ***P < 0.001. Data were displayed as mean ± SEM.

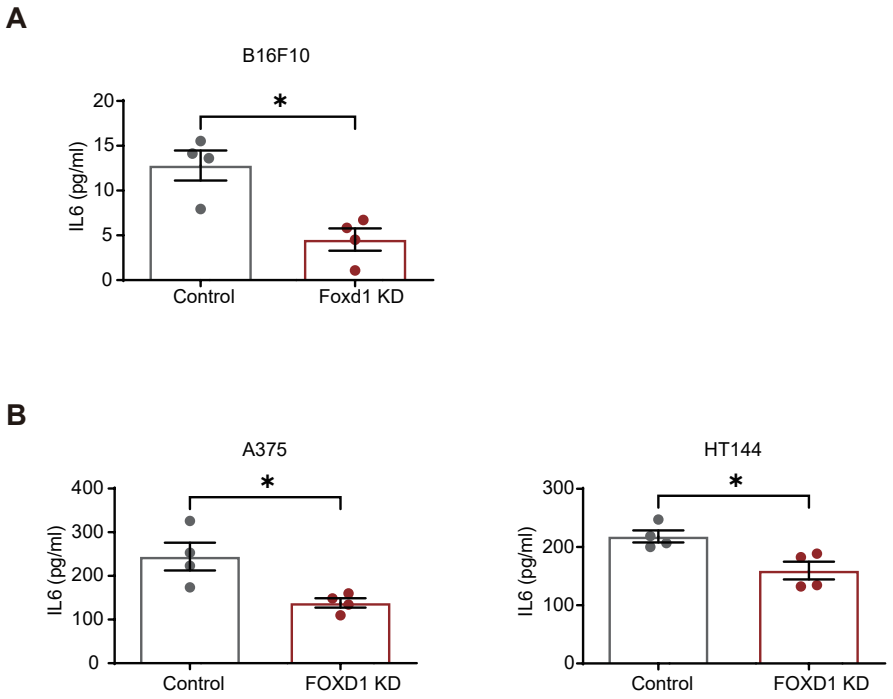

online supplemental figure 2. Regulation of IL6 expression by FOXD1.

(A) The protein level of IL6 in cond. med. from B16F10 with FOXD1 knockdown and control cells were quantified using ELISA (n=4). (B) The protein level of IL6 in cond. med. from A375 and HT144 FOXD1 KD and control cells (n=4). Statistical analysis was performed with student's two-sided t-test. *P < 0.05; **P < 0.01; ***P < 0.001. Data were displayed as mean ± SEM.

A

miRDB

Gene 2297 is predicted to be targeted by 44 miRNAs in miRDB.

Target Detail	Target Rank	Target Score	miRNA Name	Gene Symbol	Gene Description
Details	1	91	hsa-miR-581	FOXD1	forkhead box D1
Details	2	90	hsa-miR-30b-5p	FOXD1	forkhead box D1
Details	3	90	hsa-miR-30c-5p	FOXD1	forkhead box D1
Details	4	90	hsa-miR-30a-5p	FOXD1	forkhead box D1
Details	5	90	hsa-miR-30d-5p	FOXD1	forkhead box D1

B

TargetScanHuman Prediction of microRNA targets Release 8.0: September 2021

Position 518-525 of FOXD1 3' UTR

hsa-miR-581

```
5'   ...AUGGUUAACAUGUUUACACAAGA.
                    |||||||
3'            UGACUAGAUCUCUUGUGUUCU
```

C

miR-581vs mir-NC(microarray - IPA analysis)_HT144

Top Upstream Regulators

Upstream Regulators

Upstream Regulator	p-value of overlap	Predicted Activation
beta-estradiol	2.29E-26	
TP53	1.73E-23	Inhibited
MITF	4.35E-23	Activated
TGFB1	9.22E-22	
dexamethasone	8.47E-20	

FOXD1OE vs control (microarray-IPA analysis)_HT144

Top Upstream Regulators

Upstream Regulators

Upstream Regulator	p-value of overlap	Predicted Activation
KIAA1524	2.36E-06	
TP53	2.97E-06	Activated
HIF1A	4.28E-06	
TGFB1	8.26E-06	
MITF	2.59E-05	Inhibited

	FOXD1 level	MITF
FOXD1 OE	increased	inhibited
miR-581	decreased	activated

online supplemental figure 3. miR-581 acts as a potential inhibitor of FOXD1.

(A) (B) Identification of miR-581 as a potential inhibitor of FOXD1 expression with the help of the online tools, miRDB and TargetScanHuman. (C) IPA analysis was employed to predict potential biological differences between FOXD1 inhibition (using miR-581 mimics) and FOXD1 OE. Initially, a list of genes that exhibited differential expression between the miR-581 mimics and the mimics control group, as well as between the FOXD1 OE and control group of HT144 cells, was analyzed using Chipster. Subsequently, IPA was applied to compare changes in biological processes of miR-581 mimics treatment and FOXD1 OE melanoma cells in comparison with their relative controls.

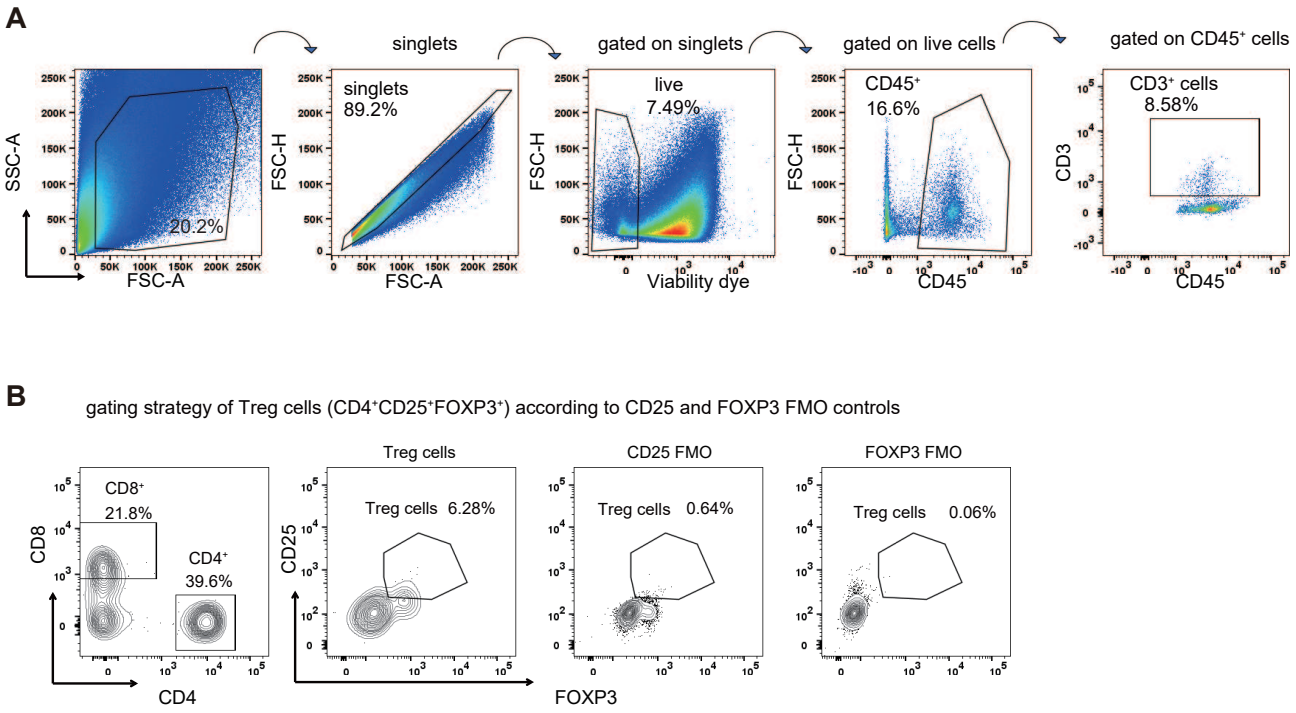

online supplemental figure 4. Gating strategy of Treg *in vivo*.

(A) PBMCs in tumor were gated first on viability and on $CD45^+CD3^+$ cell population. (B) Treg were defined by high expression of CD25, and intracellular FOXP3 among $CD4^+$ T cells.

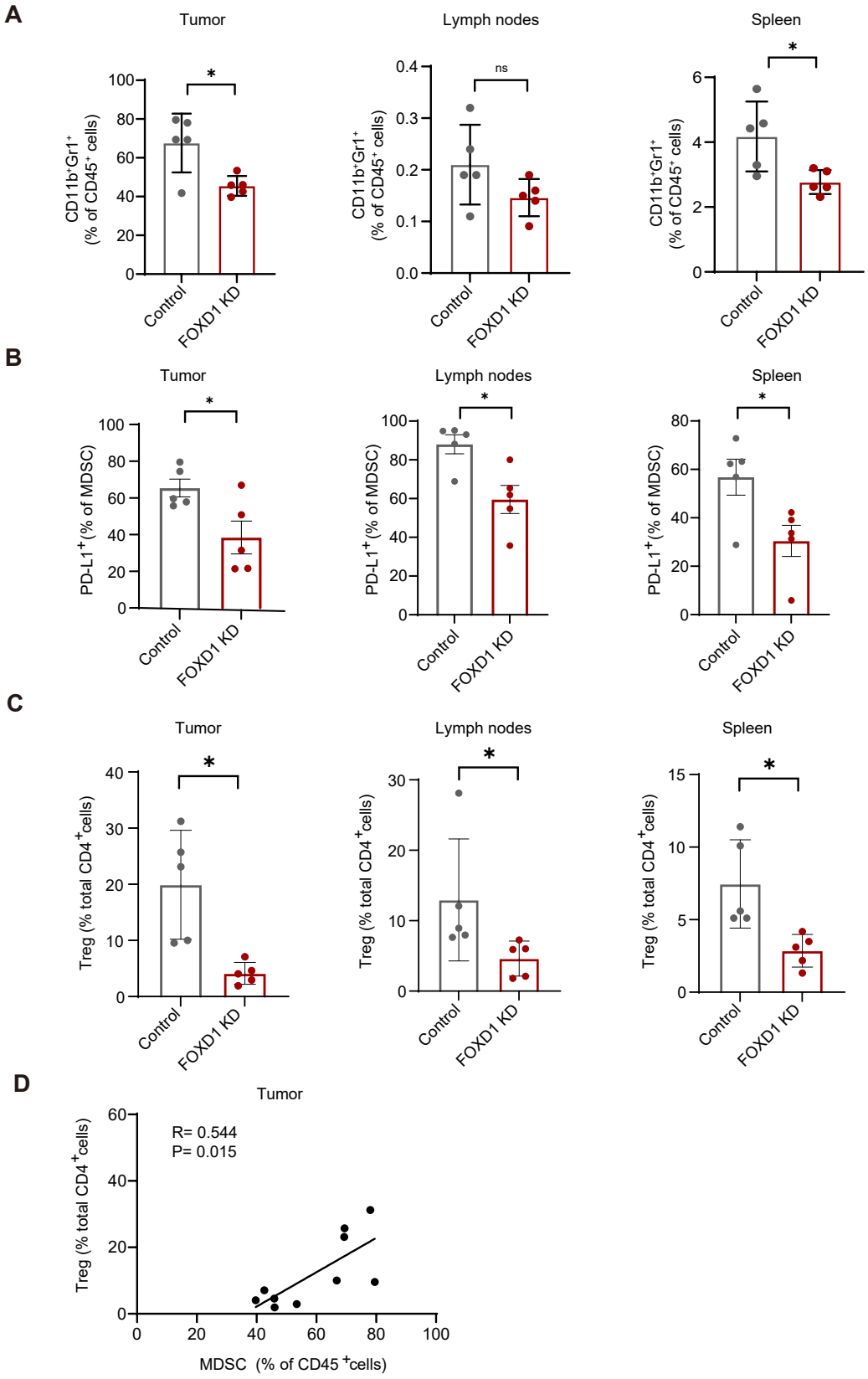

online supplemental figure 5. FOXD1 expression modulates MDSC accumulation in melanoma microenvironment.

(A) The frequency of MDSC, defined as CD11b$^+$Gr1$^+$cells among CD45$^+$ leukocytes, was compared between FOXD1 KD and control groups in spleen, lymph nodes, and tumor samples (n=5). (B) The proportion of PD-L1$^+$ cells among the total MDSC was quantified in the spleen, lymph nodes, and tumors from FOXD1 KD and control mice (n=5). (C) Treg populations, defined as CD4$^+$CD25$^+$Foxp3$^+$cells among total CD4$^+$ T cells, were measured in the spleen, lymph nodes, and tumors from both FOXD1 KD and control groups (n=5). (D) The frequency of Treg among total CD4$^+$ cells was plotted against the percentage of MDSC within CD45$^+$ leukocytes in tumors from individual mice (n=10). The correlation was evaluated by a linear regression analysis. Statistical analysis was performed with student's two-sided t-test. *P < 0.05; **P < 0.01; ***P < 0.001. Data were displayed as mean ± SEM.